

Received: 17 April 2023 / Accepted: 12 June 2023 / Published online: 14 June 2023

*surface roughness, cutting force,  
vibration, SKH2 steel, grinding*

Long HOANG<sup>1\*</sup>,  
Linh Tuan NGUYEN<sup>2</sup>

## **ANALYSING THE IMPACT OF CUTTING FORCE AND VIBRATION ON SURFACE ROUGHNESS IN EXTERNAL CYLINDRICAL GRINDING OF SKH2 STEEL**

The surface roughness of a part during external cylindrical grinding is directly impacted by cutting force and vibration, which are intermediate parameters. To improve the quality of finished parts, studying and controlling these parameters is essential. In this research, the Taguchi method combined with ANOVA analysis was utilized to analyse the effects of feed rate, cutting depth, and rotational speeds on cutting force and vibration amplitude. The test material used was SKH2 steel, which was heat-treated to a hardness of 60 HRC. The research aimed to investigate the relationship between cutting force, vibration, and surface roughness. The study concludes with an analysis of the influence of cutting force and vibration on the surface roughness of parts during external cylindrical grinding. The results show that as cutting force and vibration increase, the surface roughness of the workpiece in external grinding will also increase, and conversely when cutting force and vibration decrease, the surface roughness will decrease.

### **1. INTRODUCTION**

Cylindrical machine elements, particularly those made of high-hardness materials such as steel SKH2, are typically subjected to external cylindrical grinding to achieve the necessary surface finish. To achieve high-quality surface finishes, controlling the various factors that affect the machining process is crucial, with cutting force and vibration being two particularly important considerations.

Cutting force during external cylindrical grinding is influenced by some factors, including the cutting mode, workpiece material, and grinding wheel. This force can lead to vibrations and changes in temperature on both the workpiece and cutting tool, ultimately affecting surface roughness and size errors in the machine elements. Cutting force can be broken down into three components [1]: axial force ( $F_a$ ), which coincides with the toolpath; normal force ( $F_n$ ), which prevents the penetration of abrasive particles into the material being cut and is perpendicular to the cutting surface of the grinding wheel; and tangential force ( $F_t$ ), which acts on the grinding wheel surface.

---

<sup>1</sup> School of Mechanical Engineering, Hanoi University of Science and Technology, Vietnam

<sup>2</sup> Faculty of Mechanical Engineering, Hanoi University of Industry, Vietnam

\* E-mail: long.hoang@hust.edu.vn

<http://doi.org/10.36897/jme/168240>

Prior research has explored aspects of the shear force problem, with one study using experimental design methods to measure normal and shear force while grinding the outer circle and developing a dependent relationship between cutting force and cutting mode [2]. Another study analysed wheel topography and grit force to model grinding [3].

Vibration is a complex factor during machining, with low-intensity vibrations having minimal impact on the process. High-intensity vibrations, however, can have several negative impacts, including the formation of waves on the machined surface, reduced workpiece accuracy, increased surface roughness, greater tool wear, increased noise, and reduced machine life [4, 5]. Vibrations that occur during grinding can be either forced or self-excited, with the former resulting from misaligned machine parts and unstable movement, while the latter involves periodic relative motion between the cutting tool and workpiece that alters frictional conditions, causing microwaves and undulations on the machined surface [6].

In prior studies [7, 8], researchers have used the fast analysis Fast Fourier Transform method to analyse the vibration of the dynamic system and develop vibration models during grinding. HOANG T.-D. et al. [9] present a study to minimize values of  $Ra$  and  $Rz$  and the maximum value of material removal rate when external cylindrical grinding by the preference selection index method for input parameters including workpiece speed, feed rate, and depth of cut. BHAVSAR T. et al. [10] presented the optimization process of the cylindrical grinding of the EN353 steel by an aluminum oxide grinding wheel by selecting input parameters, including wheel speed, feed rate, and depth of cut. SINGLA S. et al. [11] studied on optimization of cylindrical grinding process parameters for heat-treated AISI 4150 steel material removal rate; the input parameters, including wheel speed, abrasive grain size, and depth of cut, were selected. Do D.-T. [12] presents a study on the multi-criteria decision-making in the external cylindrical grinding process of 65G steel. Five parameters were used to design the experimental matrix: workpiece velocity, feed rate, depth of cut, dressing feed rate, and dressing depth of cut.

Some studies have used experimental methods to measure vibration amplitude during external cylindrical grinding and establish the dependent relationship between vibration and cutting mode. In this paper, we aim to examine cutting force and vibration during external cylindrical grinding, with a specific focus on the effect of these factors on surface roughness when round grinding outside SKH2 steel.

## 2. MATERIAL AND METHODS

The experimental design method is applied to investigate the effects of cutting force and vibration on surface roughness during external cylindrical grinding. The experiments are performed using a MEG-120 cylindrical grinding machine shown in Fig. 1, with a grinding wheel that rotates at a constant speed of 2000 rpm and a workpiece speed of up to 650 rpm. The machine table has a step-less moving speed ranging from 0.1 to 5 m/min. The grinding wheel used in the experiments has dimensions of 400×50×203 and is made of corundum with a grinding grain particle size ranging from 90 to 63  $\mu\text{m}$ . A 3-grain diamond stone repairing tool with a size of 8.5×40 is also used, and the cooling method is flood cooling. The workpieces used in the experiments are designed with diameters of 40 mm, and the length

of grinding along the axis of the workpiece is 70 mm. The processing material used is SKH2 steel treated at a high temperature to achieve a hardness value of 60HRC.

Table 1. Steel brand used for experiments [13, 14]

Material	Chemical composition (%)
SKH2	C 0.7-0.8, Si $\leq$ 0.4, Mn $\leq$ 0.4, Cr 3.8–4.4, V 1-1.4, W 17.5-19



Fig. 1. External cylindrical grinding machine MEG–112

## 2.1. CUTTING FORCE MEASUREMENT METHOD

The workpieces in this study are mounted on two centre points equipped with resistive sensors. The input signal for the sensors is the real force, and the output signal is measuring force. The difference in impedance causes the Wheatstone bridge circuit to become unbalanced, generating a voltage signal of a few millivolts (mV). This small voltage signal is then amplified thousands of times to make it strong enough to be sent to an Analog-to-Digital Converter (ADC). The ADC encodes the signal, and the resulting data is stored in a computer for analysis. The computer provides reliable technical data that meet manufacturing requirements, as depicted in Fig. 2.

The cutting force during the grinding of SKH2 steel with a hardness value of 60 HRC was investigated. Based on surveys of experimental ranges of grinding modes suitable for finish grinding [2]. The feed rate ( $S_d$ ) was varied at three levels: 0.3, 0.4, and 0.5 mm/rev. The workpiece speed ( $n_w$ ) was set at three levels: 100, 150, and 200 rpm, and the cutting depth ( $t$ ) was varied at three levels: 0.005, 0.01, and 0.02 mm. The cutting forces in two components,  $F_n$  and  $F_t$ , were measured three times. The experimental design was based on the Taguchi L9 orthogonal table, which is presented in Table 2 [15].

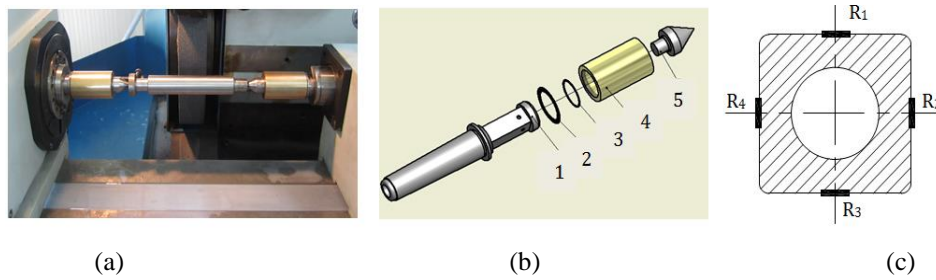


Fig. 2. Force measurement system installed on the cylindrical grinding machine [2], (a) The workpiece is secured onto the grinding machine for testing, (b) A sensor is mounted on the centre point of the workpiece, covered by grommets, and housed within a sensor ampoule (1 – Sensor body; 2,3 – Grommets; 4 – Sensor ampoule; 5 – Centre point), (c) A position stamp is marked on the deformed element for analysis

Table 2. Cutting force measurements based on Taguchi table L9 experiment

No	$S_d$ (mm/rev)	$N_w$ (rpm)	$t$ (mm)	Order of measurement times							
				$F_{n1}$ (N)	$F_{n2}$ (N)	$F_{n3}$ (N)	$\bar{F}_n$ (N)	$F_{r1}$ (N)	$F_{r2}$ (N)	$F_{r3}$ (N)	$\bar{F}_t$ (N)
1	0.3	100	0.005	6.30	6.14	6.23	6.22	1.84	2.02	2.11	1.99
2	0.3	150	0.01	6.58	7.02	7.11	6.90	2.42	2.68	2.57	2.56
3	0.3	200	0.02	11.75	12.11	11.99	11.95	4.29	4.54	4.64	4.49
4	0.4	100	0.01	10.27	10.01	10.21	10.16	3.14	4.01	4.32	3.82
5	0.4	150	0.02	16.02	15.89	15.91	15.94	5.65	5.46	5.55	5.55
6	0.4	200	0.005	9.44	9.45	9.64	9.51	3.87	3.99	3.91	3.92
7	0.5	100	0.02	22.71	22.25	21.99	22.32	7.22	7.10	7.34	7.22
8	0.5	150	0.005	13.75	13.79	13.67	13.74	4.36	4.45	4.12	4.31
9	0.5	200	0.01	15.67	15.55	15.43	15.55	5.45	5.23	5.35	5.34

## 2.2. VIBRATION MEASUREMENT METHOD MATHEMATICAL FORMULAS

The Bruel & Kjaer vibration measuring device used in this study includes a LAN-XI data collection module with four inputs and two frequency outputs of up to 51.2 kHz, a PULSE FFT 7770 analysis module with 1–3 channels, and an accelerometer sensor Triaxial DeltaTron Accelerometer with TEDS Type 4525-B-001 (Fig. 3).

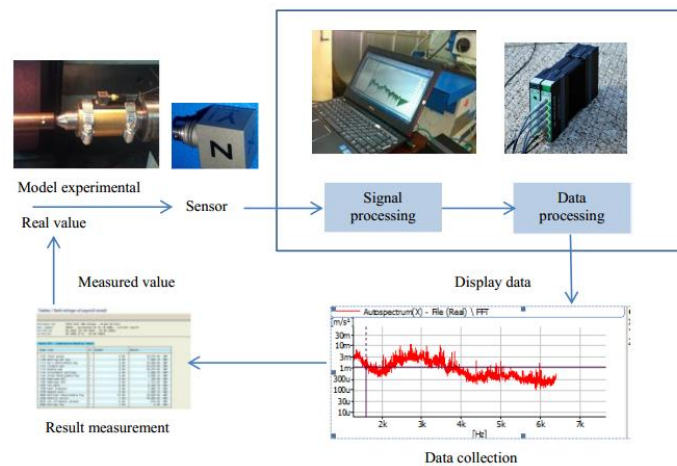


Fig. 3. Vibration measurement device

Modal analysis integrated into PULSE 17.0 software was employed to measure the vibration amplitude during machining.

The Taguchi experimental design method was utilized in this study, with three input parameters and three levels. An orthogonal L9 table was selected for the experiment, and three measurements were taken for vibration amplitude  $A$ . The resulting measurement data is presented in Table 3.

Table 3. Vibration amplitude measurements based on Taguchi table L9 experiment

No	$S_d$ mm/rev	$n_w$ rpm	$t$ mm	$A$ , m/s <sup>2</sup> (1 <sup>st</sup> )	$A$ , m/s <sup>2</sup> (2 <sup>nd</sup> )	$A$ , m/s <sup>2</sup> (3 <sup>rd</sup> )	$\bar{A}$ , m/s <sup>2</sup>
1	0.3	100	0.005	0.765	0.773	0.768	0.514
2	0.3	150	0.01	0.854	0.912	0.886	0.592
3	0.3	200	0.02	1.046	1.002	1.032	0.689
4	0.4	100	0.01	0.904	0.912	0.924	0.609
5	0.4	150	0.02	1.185	1.201	1.176	0.802
6	0.4	200	0.005	1.026	1.101	1.112	0.711
7	0.5	100	0.02	1.120	1.139	1.147	0.760
8	0.5	150	0.005	0.988	1.013	1.001	0.669
9	0.5	200	0.01	1.239	1.225	1.234	0.828

### 2.3. SURFACE ROUGHNESS MEASUREMENT METHOD

The part's surface roughness was measured using the MITUTOYO-SJ-400 surface roughness tester. The measurement was carried out three times according to the cutting force values and vibration amplitudes table. The obtained results are presented in Table 4.

Table 4. Surface roughness measurements of parts when varying cutting force and vibration amplitude

No	$\bar{F}_n$ , N	$\bar{F}_t$ , N	$\bar{A}$ , m/s <sup>2</sup>	1 <sup>st</sup> $Ra_1$ , $\mu\text{m}$	2 <sup>nd</sup> $Ra_2$ , $\mu\text{m}$	3 <sup>rd</sup> $Ra_3$ , $\mu\text{m}$	$\bar{R}_a$ , $\mu\text{m}$
1	6.22	1.99	0.514	0.29	0.31	0.32	0.31
2	6.90	2.56	0.592	0.32	0.38	0.37	0.36
3	11.95	4.49	0.689	0.54	0.60	0.61	0.58
4	10.16	3.82	0.609	0.37	0.40	0.41	0.39
5	15.94	5.55	0.802	0.50	0.45	0.52	0.49
6	9.51	3.92	0.711	0.42	0.46	0.44	0.44
7	22.32	7.22	0.760	0.52	0.55	0.54	0.54
8	13.74	4.31	0.669	0.35	0.35	0.33	0.34
9	15.55	5.34	0.828	0.53	0.52	0.56	0.54

## 3. RESULT AND DISCUSSIONS

For analyzing the influence of cutting mode parameters on the cutting force, the signal factor ( $SN_i$ ) is used, as expressed in equation (1):

$$SN_i = -10 \log \left( \sum_{u=1}^{N_i} \frac{y_u^2}{N_i} \right) \tag{1}$$

where  $i = 1$  to 9,  $u$  represents the number of tests ( $u = 1$  to 3), and  $N_i$  represents the number of trials for experiment  $i$  ( $N_i = 3$ ).

The calculated signal factor ( $S.N.$ ) was used to evaluate the influence of each cutting mode parameter on the cutting force. The  $S.N.$  values for each parameter are presented in Table 5.

Table 5. Signal factors ( $S.N.$ ) showing the degree of influence of experimental parameters on cutting force

Level	$F_n$			$F_t$		
	$S.N.$ calculated for $S_d$	$S.N.$ calculated for $N_w$	$S.N.$ calculated for $t$	$S.N.$ calculated for $S_d$	$S.N.$ calculated for $N_w$	$S.N.$ calculated for $t$
1	-17.9989	-21.0105	-19.3989	-9.07011	-11.6301	-10.2012
2	-21.1993	-21.2011	-20.2401	-12.7994	-11.8997	-11.5002
3	-24.4989	-21.6501	-24.1904	-14.7997	-13.1598	-15.1007
R	6.3998	0.6492	4.7905	5.7398	1.5297	4.8498

Using ANOVA (Analysis of Variance) analysis to evaluate the influence of each main parameter and the interactive effects of parameters on the cutting force, we obtained the results as shown in Figs. 4, 5, 6, and 7.

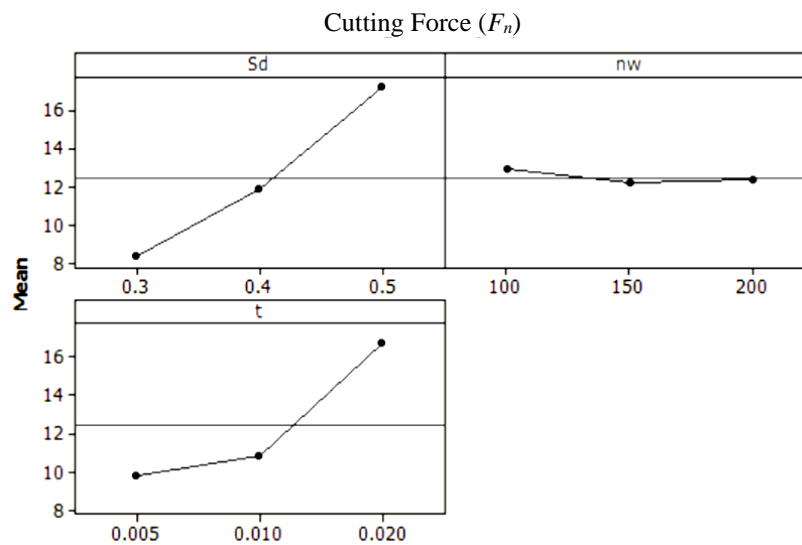


Fig. 4. Graphical representation of the influence of each main parameter ( $S_d, n_w, t$ ) on the  $F_n$ .

Based on the data presented in Table 5 and Figs. 4, 5, 6, and 7, the study reveals that feed rate and cutting depth are the parameters that have a significant impact on the cutting forces  $F_n$  and  $F_t$ , while the effect of workpiece speed is relatively low. The cutting force increases with an increase in feed rate and cutting depth and decreases when the feed rate and cutting depth decrease. The feed rate and cutting depth interactions are the most prominent at  $S_d = 0.5$  and  $t = 0.2$ .

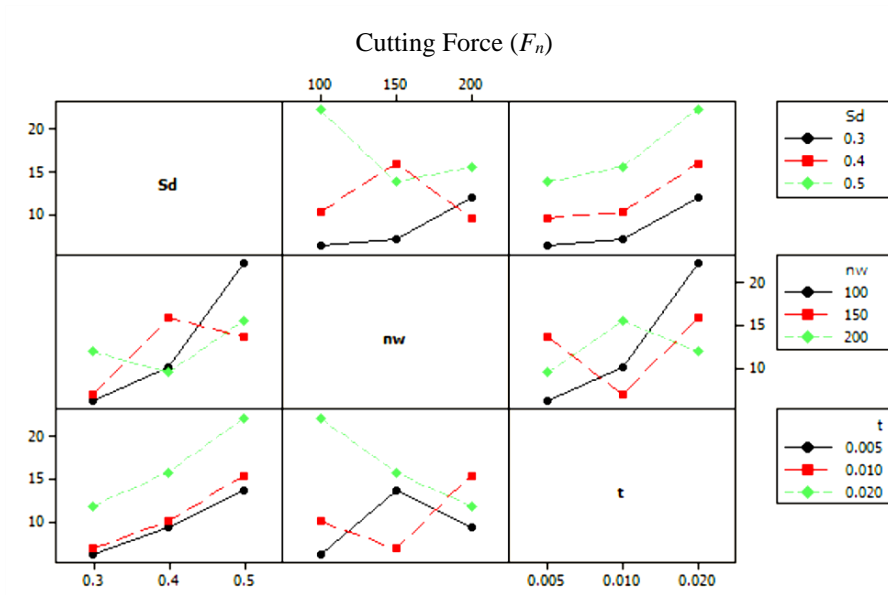


Fig. 5. Graph of interactive effects of parameters ( $S_d, n_w, t$ ) on the  $F_n$

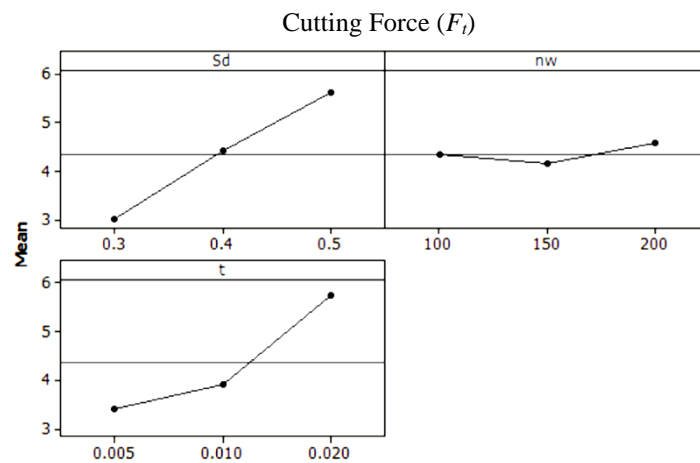


Fig. 6. Graphical representation of the influence of each main parameter ( $S_d, n_w, t$ ) on the  $F_t$

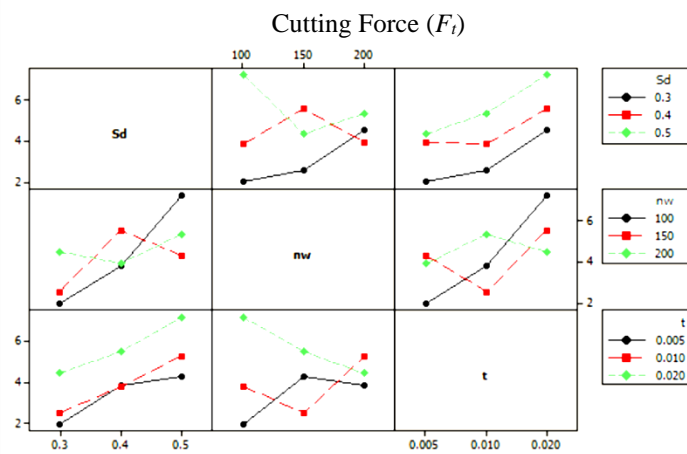


Fig. 7. Graph of interactive effects of parameters ( $S_d, n_w, t$ ) on the  $F_t$

The calculated *S.N.* for each parameter to evaluate their influence on the vibration amplitude is shown in Table 6.

Table 6. Degree of influence of experimental parameters on vibration amplitude

Level	A		
	<i>S.N.</i> calculated for $S_d$	<i>S.N.</i> calculated for $N_w$	<i>S.N.</i> calculated for $t$
1	1.0410	0.6565	0.5359
2	-0.4586	-0.1434	0.0126
3	-0.9753	-0.9060	-0.9416
R	2.0164	1.5625	1.4775

Using ANOVA analysis to evaluate the influence of each main parameter (feed rate, workpiece speed, and cutting depth) and interactive effects of parameters on the cutting force, the results were obtained and presented in Figs. 8 and 9.

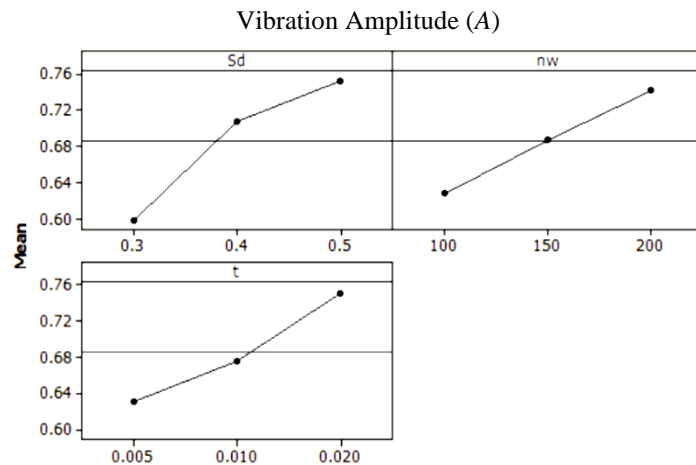


Fig. 8. Graphical representation of the influence of each main parameter ( $S_d, n_w, t$ ) on the A

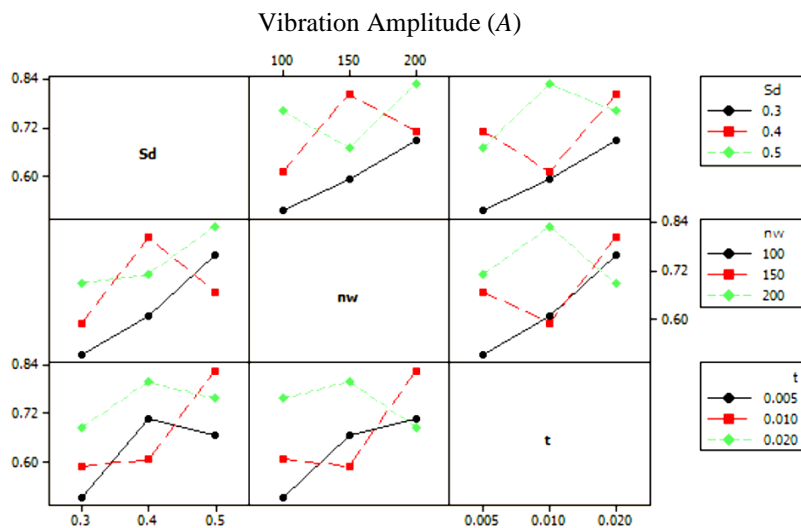


Fig. 9. Graph of interactive effects of parameters ( $S_d, n_w, t$ ) on the A

The influence of feed rate, workpiece rotation speed, and cutting depth on the vibration amplitude was evaluated using ANOVA analysis. The results are presented in Table 6 and Figs. 8 and 9. It is shown that all three parameters significantly impact the vibration amplitude, with feed rate having the greatest influence, followed by workpiece rotation speed and cutting depth. When the feed rate, workpiece rotation speed, and cutting depth increase, the vibration amplitude also increases, and vice versa.

The influence of cutting force  $F_n$ , tangential force  $F_t$ , and vibration amplitude  $A$  on surface roughness ( $Ra$ ) was analysed using ANOVA. The results of the analysis are presented in Fig. 10.

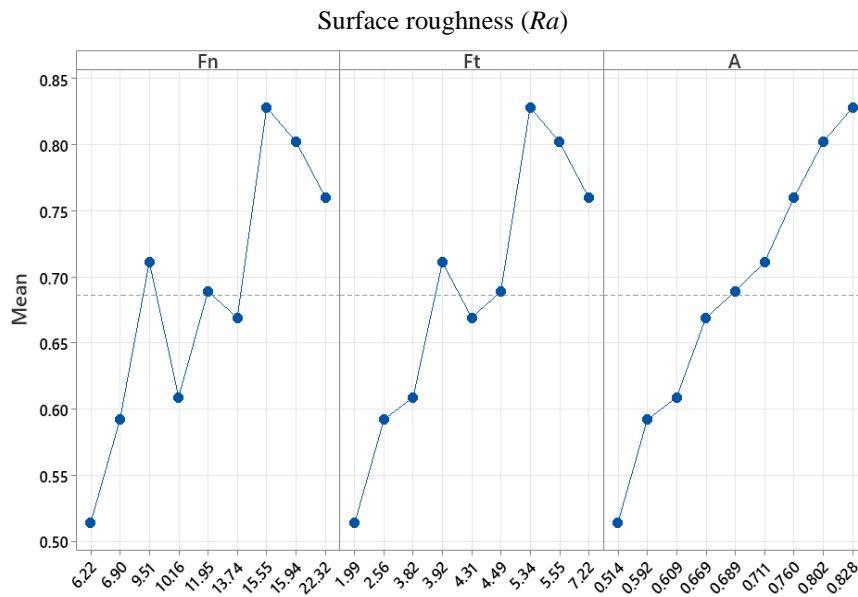


Fig. 10. Graphical representation of the influence of each main parameter  $F_n$ ,  $F_t$ , and  $A$  on  $Ra$

The surface roughness of the part was measured, and the results are presented in Table 4. Based on the experimental data, the regression equation describing the relationship between cutting force, vibration amplitude, and surface roughness was determined and is shown in equation (2):

$$Ra = 1.087F_n - 0.1637F_t - 17.67A - 0.09930F_n^2 + 0.1129F_t^2 + 40.95A^2 + 0.3665F_n \cdot F_t - 0.3720F_n \cdot A - 7.641F_t \cdot A \tag{2}$$

Figure 9 illustrates the influence of cutting force and vibration on surface roughness. The results indicate that within the range of the experiments, the increase in shear force and vibration amplitude leads to an increase in surface roughness, while decreasing the same leads to a decrease in surface roughness. Therefore, as the cutting force and vibration decrease, the workpiece will have a minor surface roughness after grinding. For reducing the cutting force, it is necessary to adjust the parameters  $S_d$  and  $t$  to their minimum values while keeping  $n_w$  at its average value. To decrease vibration, all three parameters,  $S_d$ ,  $t$ , and  $N_w$ , must be adjusted to their minimum values. However, due to the more significant influence of  $S_d$  and  $t$  compared to  $n_w$ , the optimal grinding mode within this range of investigation is achieved with  $S_d = 0.3$  mm/rev,  $t = 0.05$  mm, and  $N_w$  ranging from 100 to 150 rpm. With the grinding parameters

set as  $S_d = 0.3$  mm/rev,  $t = 0.05$  mm, and  $n_w = 100$  rpm,  $F_n = 6.22$  N,  $F_t = 1.99$  N, and  $A = 0.514$  m/s<sup>2</sup>. After substituting these values into equation (2), the predicted surface roughness value is  $Ra = 0.308$   $\mu\text{m}$ . The measured average surface roughness value is  $Ra = 0.31$   $\mu\text{m}$ . The deviation between the predicted and measured surface roughness values is 0.645%.

#### 4. CONCLUSION

In conclusion, this study aimed to investigate the impact of cutting force and vibration on surface roughness during external cylindrical grinding of SKH2 steel. The Taguchi method combined with ANOVA analysis was used to analyse the effects of feed rate, cutting depth, and rotational speeds on cutting force and vibration amplitude. Among them, the feed rate ( $S_d$ ) and cutting depth ( $t$ ) have a significant impact on cutting force, while the workpiece rotation speed ( $n_w$ ) has minimal influence. Regarding vibration, the  $S_d$  has a much greater effect compared to the other two parameters. The surface roughness of the workpiece after grinding depends on many factors; however, cutting force and vibration are important factors that need to be considered and controlled. The experimental results indicated that cutting force and vibration had significant effects on surface roughness. The findings showed that increasing the cutting force and vibration amplitude resulted in increased surface roughness. The results of this study provide valuable insights for improving the quality of finished parts in external cylindrical grinding processes. It is recommended that future research explore the influence of other parameters, such as grinding wheel characteristics and coolant type, on surface roughness during external cylindrical grinding.

#### REFERENCES

- [1] BRIAN ROWE W., 2009, *Principles of Modern Grinding Technology*, William Andrew Publishing.
- [2] NGUYEN T.-L., THAI V.-T., HOANG L., 2021, *Experimental Investigation of the Effects of Process Parameters on Cutting Force in External Cylindrical Grinding*, Tribology in Industry, 43/ 2, 274–282, <https://doi.org/10.24874/ti.1013.11.20.01>.
- [3] ROGELIO L. HECKER, IGOR M. RAMONEDA, STEVEN Y. LIANG, 2003, *Analysis of Wheel Topography and Grit Force for Grinding Process Modeling*, Journal of Manufacturing Processes, 5/1, 13–23, [https://doi.org/10.1016/S1526-6125\(03\)70036-X](https://doi.org/10.1016/S1526-6125(03)70036-X).
- [4] HAHN R.S., 1954, *On the Theory of Regenerative Chatter in Precision Grinding Operations*, Transaction of ASME, 76/4, 593–597.
- [5] SNOEYS R., BROWN D., 1969, *Dominating Parameters in Grinding Wheel and Workpiece Regenerative Chatter*, Proceedings of the 10th International Machine Tool Design and Research Conference, Manchester, 325–348.
- [6] KLOCKE F., 2009, *Manufacturing Processes 2 Grinding, Honing, Lapping*, Springer Publishing.
- [7] NEMETH STEPHAN, NESLLUSAN MIROSLA, 2007, *Vibration in Grinding Operations*, 7th International Multidisciplinary Conference, Baia Mare, Romania, 537–542.
- [8] HONGQ LI., YUNG C. SHIN, 2006, *A Time-Domain Dynamic Model for Chatter Prediction of Cylindrical Plunge Grinding Processes*, ASME Journal of Manufacturing Science Engineering, 128, 404–415, <https://doi.org/10.1115/1.2118748>.
- [9] HOANG T.-D., D.O. D.-T., NGUYEN V.-T., NGUYEN N.-T., 2021, *Multi-Objective Optimization of the Cylindrical Grinding Process of SCM440 Steel Using Preference Selection Index Method*, Journal of Machine Engineering, 21/3, 110–123, <https://doi.org/10.36897/jme/141607>.
- [10] BHAVSAR T., NOKALJE A.M., 2020, *Optimization of Cylindrical Grinding Process Parameters for EN353 Steel Using Taguchi Technique*, International Journal for Research in Applied Science & Engineering Technology, 8/11, 225–231.

- [11] SINGLA S., DEV D.K., 2018, *Optimization of Cylindrical Grinding Process Parameters for Heat Treated AISI 4150 Steel*, International Journal on Theoretical and Applied Research in Mechanical Engineering, 7/2–3, 5–10.
- [12] D.O. D.-T., 2021, *The combination of Taguchi-Entropy-Waspas-Piv Methods for multi-criteria decision making when external cylindrical grinding of 65G steel*, Journal of Machine Engineering, 21/4, 90–105, <https://doi.org/10.36897/jme/144260>.
- [13] NGUYEN T.-L., NGUYEN N.-T., HOANG L., 2020, *A Study on the Vibrations in the External Cylindrical Grinding Process of the Alloy Steels*, International Journal of Modern Physics B, 34/22n24, 1–6, <https://doi.org/10.1142/S0217979220401505>.
- [14] JOHN E. BRINGAS, 2004, *Handbook of Comparative World Steel Standards*, ASTM DS67B.
- [15] ROY K. RANJIT, 2001, *Design of Experiments Using the Taguchi Approach, 16 Steps to Product and Process Improvement*, John Wiley & Sons Inc.